

OPTICAL CONSTANTS OF SOLID METHANE

BISHUN N. KHARE,* W.R. THOMPSON,* C. SAGAN,* E.T. ARAKAWA,** C. BRUEL,**
J.P. JUDISH,** R.K. KHANNA,*** AND J.B. POLLACK†

*Laboratory for Planetary Studies, Cornell University, Ithaca, New York, 14853

**Oak Ridge National Laboratory, Oak Ridge Tennessee 37831

***Department of Chemistry and Biochemistry, University of Maryland, College Park,
Maryland 20742

†NASA Ames Research Center, Moffett Field, California 94035

ABSTRACT

Methane is the most abundant simple organic molecule in the outer solar system bodies. In addition to being a gaseous constituent of the atmospheres of the Jovian planets and Titan, it is present in the solid form as a constituent of icy surfaces such as those of Triton and Pluto, and as cloud condensate in the atmospheres of Titan, Uranus, and Neptune. It is expected in the liquid form as a constituent of the ocean of Titan. Cometary ices also contain solid methane. The optical constants for both solid and liquid phases of CH_4 for a wide temperature range are needed for radiative transfer calculations, for studies of reflection from surfaces, and for modeling of emission in the far infrared and microwave regions. The astronomically important visual to near infrared measurements of solid methane optical constants are conspicuously absent from the literature.

We present preliminary results on the optical constants of solid methane for the $0.4 \mu\text{m}$ to $2.6 \mu\text{m}$ region. Deposition onto a substrate at 10°K produces glassy (semi-amorphous) material. Annealing this material at $\sim 33^\circ\text{K}$ for ~ 1 hour results in a crystalline material as seen by sharper, more structured bands and negligible background extinction due to scattering. We report k for both the amorphous and the crystalline (annealed) states. Typical values (at absorption maxima) are in the 10^{-3} to 10^{-5} range. Below $\lambda = 1.1 \mu\text{m}$ the bands are too weak to be detected by transmission through the films $\leq 215 \mu\text{m}$ in thickness, employed in our studies to date.

Using our previously measured values of the real part of the refractive index, n , of liquid methane at 110°K [*Bull. Am. Phys. Soc.* 31, 700 (1986)] we compute n for solid methane using the Lorentz-Lorenz relationship. Values vary monotonically from $n = 1.304$ at $\lambda = 0.4 \mu\text{m}$ to $n = 1.296$ at $\lambda = 2.0 \mu\text{m}$. An independent, direct determination using interference fringes at two angles of incidence finds $n = 1.31 \pm 0.02$ for the solid film at $\lambda = 0.4\text{-}0.7 \mu\text{m}$, a value confirmed by laser interferometry.

Work is in progress to extend the measurements of optical constants n and k for liquid and solid to both shorter and longer wavelengths, eventually providing a complete optical constants database for condensed CH_4 .

INTRODUCTION

The absorption, emission, reflection and scattering of radiation by atmospheres and surfaces depends on the vertical and horizontal distribution of material, on particle size and shape, and most fundamentally on the optical characteristics of the materials present. These optical characteristics can be represented by the complex refractive index. The real and imaginary parts are commonly called the optical constants n and k , and can be determined in the laboratory by a variety of techniques.¹ CH_4 optical constants are required in radiative transfer calculations modeling light scattering and the thermal structure of planetary atmospheres, and in studies of reflection from particulate surfaces containing CH_4 ice and frost, such as those of Triton and Pluto; and also in the calculation of the energy deposition profile and penetration depth for charged particles impinging on icy outer solar system surfaces. These quantities can be calculated from the "stopping power":

$$\frac{dE}{dX} \propto \int_0^{\infty} -\text{Im} \left[\frac{1}{\epsilon(\omega)} \right] d\omega,$$

where $\epsilon = \epsilon_1 + \epsilon_2$, $\epsilon_1 = n^2 - k^2$, $\epsilon_2 = 2nk$, n and k are the real and imaginary part of the refractive index, and ω is the frequency.

We have been engaged for the last several years in the laboratory determination of complex refractive indices of materials of planetary and astronomical interest. The optical constants of Titan tholin¹ produced from ~ 90% N_2 and 10% CH_4 in a plasma discharge similar to that produced by Saturnian magnetospheric charged particles which are intercepted by Titan's upper atmosphere, were utilized in radiation transfer calculations,^{2,3,4} producing, for example, reflection spectra⁵ and thermal structure⁴ of Titan's atmosphere consistent with the ground based spectroscopic observations,⁶ with Pioneer 11 polarimetric observations;⁷ and with Voyager photometric observations.^{8,9} Successful applications were also made with optical constants of $\text{H}_2/\text{He}/\text{CH}_4$ tholin appropriate to Neptune and the Uranian troposphere.¹⁰ One of our current emphases is the determination of optical properties of condensed hydrocarbons and the effect of irradiation on these properties. Simple hydrocarbons such as methane (CH_4), ethane (C_2H_6), and acetylene (C_2H_2) are prime candidates for such studies because of their importance on several planets and their icy satellites. For example,

(a) Titan's surface probably has lakes or oceans of CH_4 and C_2H_6 , with several other minor species.^{11,12,13}

(b) C_2H_6 , and C_2H_2 form condensate hazes in the stratospheres of Uranus and Neptune.¹⁴

(c) CH_4 clouds are present on Uranus and Neptune.¹⁵

- (d) Condensed CH_4 is present on both Triton¹⁶ and Pluto^{17,18} and
- (e) The presence of CH_4 in cometary comae¹⁹ suggests the presence of condensed CH_4 and probably other hydrocarbon ices there.

A critical survey of the literature reveals that the availability of optical constants data for these materials in the visible-near IR region ranges from sparse to totally absent. We present below some preliminary results of the measurements of optical constants of solid CH_4 in the $1.1 \mu\text{m}$ to $2.6 \mu\text{m}$ range, and calculations of k and a tabulation of n throughout the visible and near-infrared.

EXPERIMENTAL DETAILS AND RESULTS

Sample Preparation

The solid films of methane were made by pulse deposition of gaseous methane on a substrate attached to the cold finger of a commercial cryocooler²⁰ as shown in Figure 1. An externally controlled heater wound around the cold finger of the

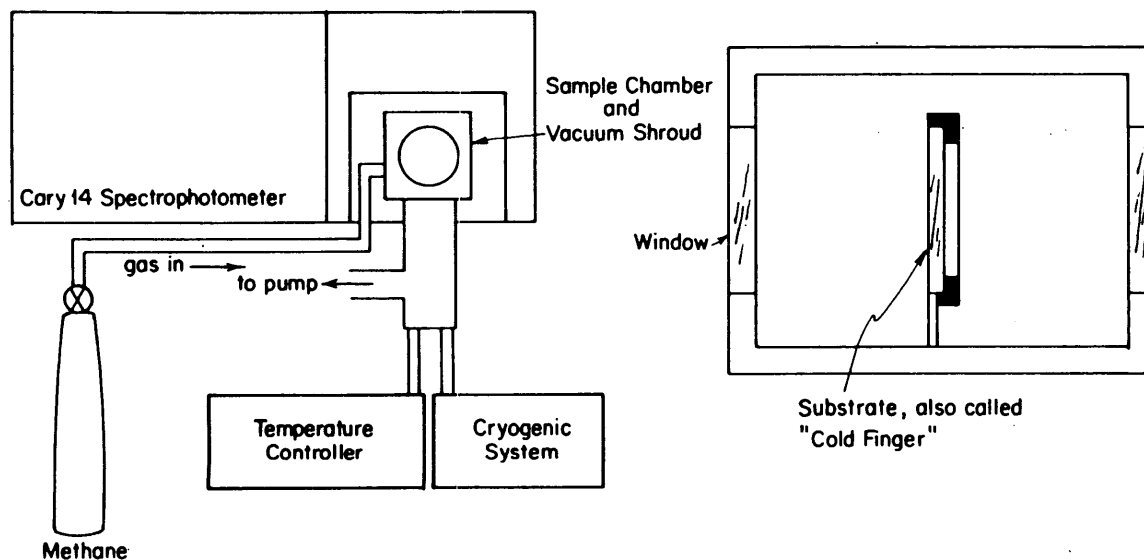


Fig. 1. Experimental set-up to measure transmission through methane film at 10°K

cryocooler enabled us to control the sample temperature to within $\pm 0.5^\circ\text{K}$. Both KRS-5 (for transmission) as well as polished silicon (for reflectance) were employed as substrates. Typically, the sample was deposited at 10°K which resulted in amorphous films, as evidenced by broad structureless bands in the infrared region (Figure 2). Annealing the sample at $\sim 33^\circ\text{K}$ for approximately an hour resulted in crystallinity, as evidenced by sharper structured bands and negligible background extinction due to

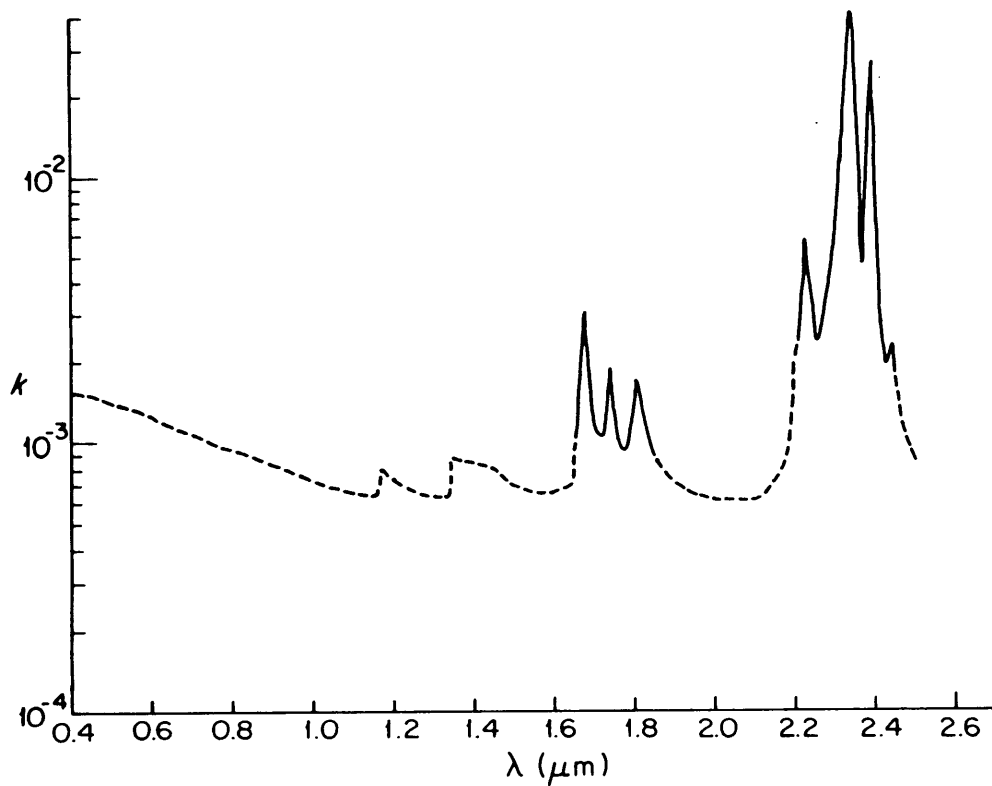


Fig. 2. Freshly deposited glassy (semi-amorphous) film of methane at $\sim 10^\circ\text{K}$

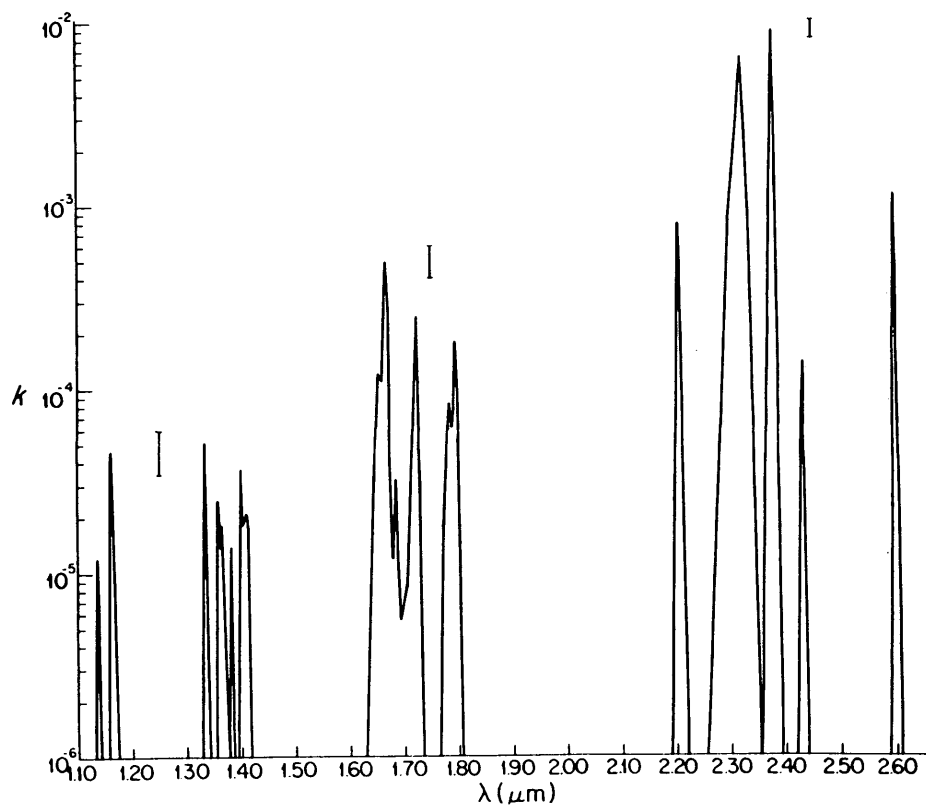


Fig. 3. Crystalline film of methane at $\sim 33^\circ\text{K}$ after annealing for ~ 1 hour

scattering (Figure 3). Several films from 5 μm to 215 μm thickness were investigated.

Spectral Measurements

The spectra were recorded on a Cary-14 UV-VIS-NIR spectrometer from 0.35 μm to 2.5 μm with a spectral resolution $\sim 6\text{ cm}^{-1}$. The region 2.0 μm to 2.6 μm was also measured with a Perkin-Elmer 1800 FTIR spectrometer at $\sim 1\text{ cm}^{-1}$ resolution.

Data Analysis

Imaginary part of the refractive index k

The determination of the imaginary part of the refractive index, k , is determined directly by measuring the transmission through a film of thickness t and using the relation,

$$k = \frac{\lambda}{4\pi t} \ln \frac{T_s (1-R)}{T (1-R_0)^2} \quad (1)$$

where T = transmission, T_s = Transmission of the substrate alone,

$$R_0 = \left(\frac{n_s - 1}{n_s + 1} \right)^2$$

and n_s = the real part of the refractive index of the substrate, known from independent measurements or from the literature.²¹ R = the total reflectance of the film and substrate, which can be approximately determined by constructing a baseline through points where the film has no absorption bands. Further details are given by Khare et al.¹

The only unknown in Equation (1) is the thickness of the film t which we determine from the interference fringes at 0.35 μm to 0.75 μm for two angles of incidence.²² Since the absorption in this region is very small, the real part of the refractive index does not undergo any appreciable dispersion. Assuming n to be constant, the two equations

$$2t (n^2 - \sin^2\theta_1)^{1/2} = \Delta N \left(\frac{\lambda_1\lambda_2}{\lambda_1 - \lambda_2} \right)$$

and

$$2t (n^2 - \sin^2\theta_2)^{1/2} = \Delta N \left(\frac{\lambda_3\lambda_4}{\lambda_3 - \lambda_4} \right) \quad (2)$$

where ΔN is the number of fringes in the range $(\lambda_1 - \lambda_2)$ and $(\lambda_3 - \lambda_4)$ for the two angles of incidence θ_1 and θ_2 respectively, can be solved for n and t . The thickness of the film can be obtained within about 2-5% accuracy for 5-30 μm thick films. For the

thickest film (215 μm) employed in our work, the fringes are too close to be separated accurately. For this sample, the thickness was estimated from the integrated band intensities of the stronger peaks and from the knowledge of the extinction coefficient of these bands measured for thinner films.

Substituting for t in Eq. (1) yields the k values for crystalline CH_4 tabulated in Table 1 and plotted in Figure 3.

The k values calculated for the amorphous film of methane are plotted in Figure 2. These results are of much poorer quality than those for crystalline CH_4 because of large background scattering. If the background contribution is subtracted from the observed data, then the k values for amorphous methane are approximately the same magnitude as the corresponding k values for crystalline methane. As we go towards wavelengths shortward of $\lambda = 1.6 \mu\text{m}$ (Figure 2) into the visible, the loss of photons due to scattering dominates over the loss due to absorption at the peaks to such an extent that one finds complete loss of absorption features. The k values at peaks for solid glassy amorphous film are higher than those of the corresponding peak values of the crystalline film at $\sim 33^\circ\text{K}$ because of the background scattering by the non-crystalline sample.

For crystalline CH_4 (a 215 μm thick sample), scattering is much less of a problem, allowing determination of values of k as small as 10^{-6} down to a wavelength of 1.1 μm .

Extinction in solid CH_4 in the VIS-NIR region (0.4-1.1 μm) is expected to be extremely small ($k < 10^{-6}$). In Figure 4 we plot k for liquid CH_4 ^{23,24} (solid line) measured by Ramaprasad²³ et al. and Patel²⁴ et al. and the k values computed²⁵ from room-temperature gas data obtained by Giver²⁶ if taken to a liquid density of 0.45 g cm^{-3} (dashed line). At low resolution, both the experimentally measured liquid CH_4 k values and those computed from gas data, are similar (Figure 4), and therefore temperature and density effects for CH_4 are minor in the VIS-NIR ($\lambda < 1.1 \mu\text{m}$). Since CH_4 retains rotational freedom in the solid state, only minor liquid-solid spectral differences are expected.²⁵ Figure 4 therefore provides a good guide for attempts to measure k in the solid at visual wavelengths. We are attempting to make optical quality solid methane discs varying in thickness from 1 to 10 μm , but Figure 4 would indicate that much thicker samples of the order of a meter or so are required to obtain k data in this region. This work is continuing at present, along with investigations of weak interband absorption and some work on other hydrocarbons.

The measurement accuracy for the crystalline CH_4 results of Figure 3 and Table I is about $\pm 5\%$, and is indicated by error bars on the graph. The largest single source of error is uncertainty in the correction of absorbance measurements on the Cary-14 spectrometer, which deviate from linearity at the higher end of the 0-1 absorbance scale. The value of k determined from the data taken on the P.E. 1800 FTIR

Table I

Imaginary Part of the Refractive Index (k) at Various Wavelengths (λ) of a Crystalline Film of CH_4 at $\sim 33^\circ\text{K}$

λ (μm)	$k = a \cdot 10^{-b}$		λ (μm)	$k = a \cdot 10^{-b}$		λ (μm)	$k = a \cdot 10^{-b}$	
	a	b		a	b		a	b
1.133	1	>6	1.415	1.7	5	1.789	6.2	5
1.138	1.9	5	1.418	1	>6	1.792	7.8	5
1.143	1	>6	1.629	1	>6	1.796	1.8	4
1.156	1	>6	1.646	3.0	5	1.799	8.4	5
1.162	1.9	5	1.652	7.7	5	1.803	1.5	5
1.163	4.6	5	1.655	1.2	4	1.806	1	>6
1.164	4.7	5	1.660	1.1	4	1.830	1	>6
1.169	9.8	6	1.664	1.7	4	2.191	1	>6
1.171	9.8	6	1.669	5.0	4	2.207	7.9	4
1.173	1	>6	1.672	2.8	4	2.220	1	>6
1.330	1	>6	1.675	3.9	5	2.254	1	>6
1.333	2.4	5	1.683	1.2	5	2.299	8.4	4
1.336	5.3	5	1.687	2.8	5	2.323	6.4	3
1.341	1	>6	1.690	1.1	5	2.335	9.5	4
1.355	1	>6	1.694	5.6	6	2.353	1	>6
1.359	2.5	5	1.706	8.6	6	2.374	9.6	4
1.364	1.4	5	1.717	5.1	5	2.380	9.0	3
1.365	1.8	5	1.719	7.4	5	2.383	1.3	3
1.378	1	>6	1.723	2.5	4	2.393	1	>6
1.383	1.4	5	1.728	3.7	5	2.419	1	>6
1.387	1	>6	1.731	5.8	6	2.431	1.4	4
1.394	1	>6	1.735	1	>6	2.439	1	>6
1.402	3.7	5	1.766	1	>6	2.589	1	>6
1.405	1.9	5	1.773	1.8	5	2.600	1.1	3
1.407	1.9	5	1.778	3.8	5	2.608	1	>6
1.410	2.1	5	1.785	8.3	5			

are good to around $\pm 10\%$, with most of the error coming from the estimate of the $215 \mu\text{m}$ -thick sample.

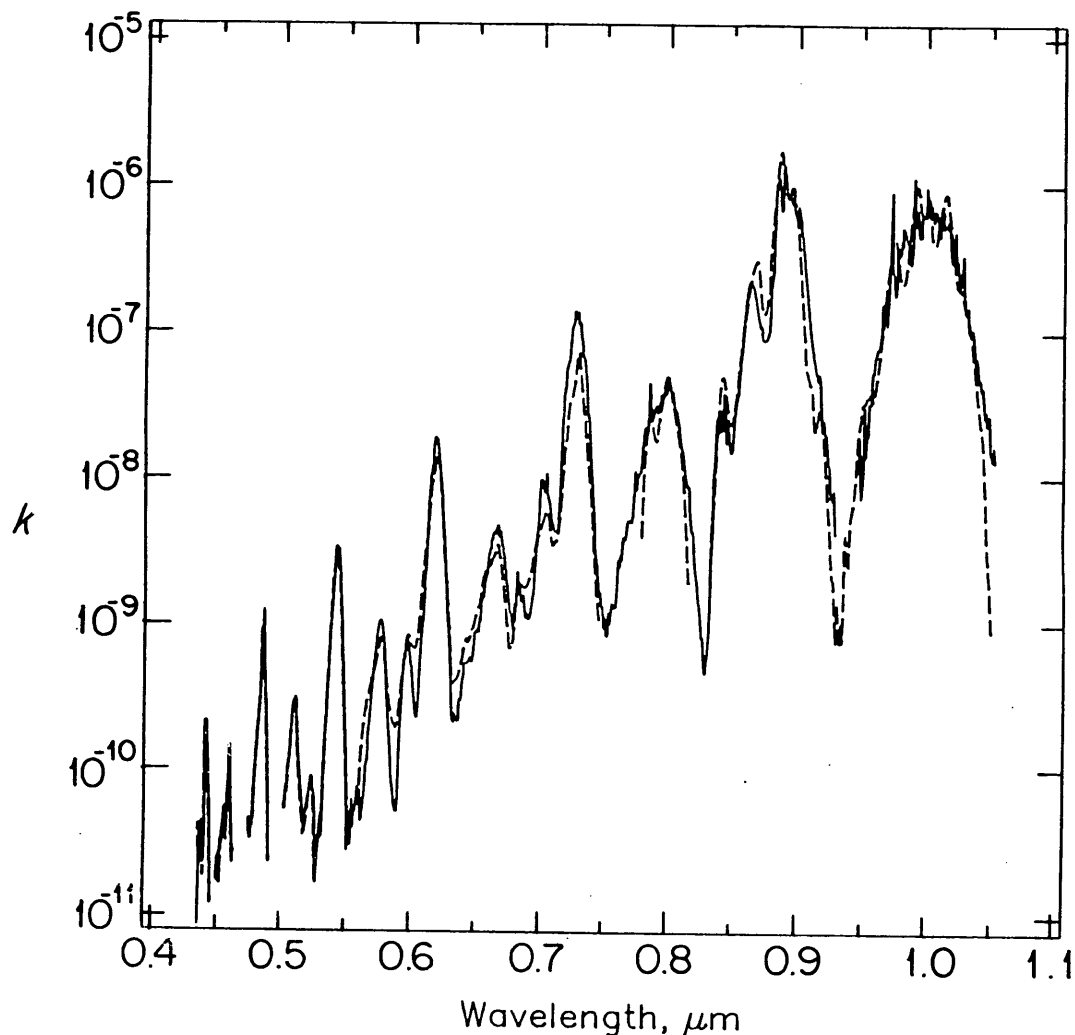


Fig. 4. Comparison²⁵ of k of liquid CH_4 ^{23,34} (dashed line) with computed k values from room temperature gas data²⁶ if taken to a liquid density of 0.45 g cm^{-3} (solid line). Values are similar everywhere, and nearly indistinguishable below $0.55 \mu\text{m}$.

Real part of the refractive index n

Using the technique of ellipsometric polarimetry, we have measured the refractive indices of liquid methane²⁷ at $\sim 110^\circ\text{K}$ from $\lambda = 0.4$ to $\lambda = 2.0 \mu\text{m}$. Using the Lorentz-Lorenz relationship

$$\frac{n_s^2 - 1}{n_s^2 + 2} \bigg/ \frac{n_l^2 - 1}{n_l^2 + 2} = d_s/d_l \quad (3)$$

where subscripts l and s represent the liquid and solid phases of CH_4 respectively, we could estimate the real part of the refractive index knowing the densities of liquid and solid CH_4 . The density²⁸ of liquid CH_4 at 110°K is $0.42441 \text{ g cm}^{-3}$. The density of solid CH_4 , $d_s = 0.449 \text{ g cm}^{-3}$ at the temperature of our solid film, $\sim 20^\circ\text{K}$. This density is obtained by extrapolating the values of Constantino and Daniels.²⁹ n values calculated by using Lorentz-Lorenz relationship [Eq. (3)] are given in Table II and are in good agreement with the value of $n = 1.31 \pm 0.02$ calculated from interference fringes we obtained during reflection measurements for two angles of incidence (Eq. 2).

Table II

Real Part of the Refractive Index n_s of Solid Methane Calculated from Lorentz-Lorenz Relationship						
λ (μm)	0.4	0.6	0.8	1.0	1.2	2.0
n_l	1.286	1.283	1.281	1.280	1.280	1.278
n_s	1.304	1.301	1.299	1.298	1.298	1.296

n for solid methane at $\lambda = 0.6328 \mu\text{m}$ was further confirmed independently by a dual angle laser interference technique³⁰ employed to monitor film thickness and the refractive index. Two He-Ne laser beams were specularly reflected off a polished silicon crystal which was used as a substrate (Fig. 5).

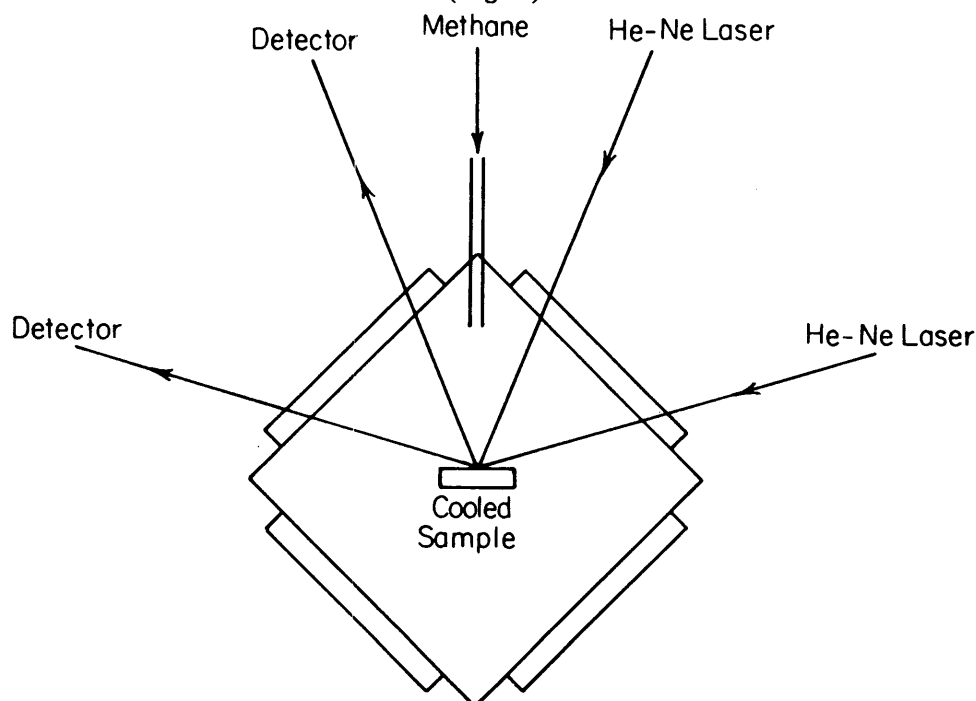


Fig. 5

As the methane gas is condensed at a constant rate, two interference patterns of different periods are recorded in the reflected laser light as a function of film thickness (Fig. 6). If the ratio of separation between adjacent maxima in two

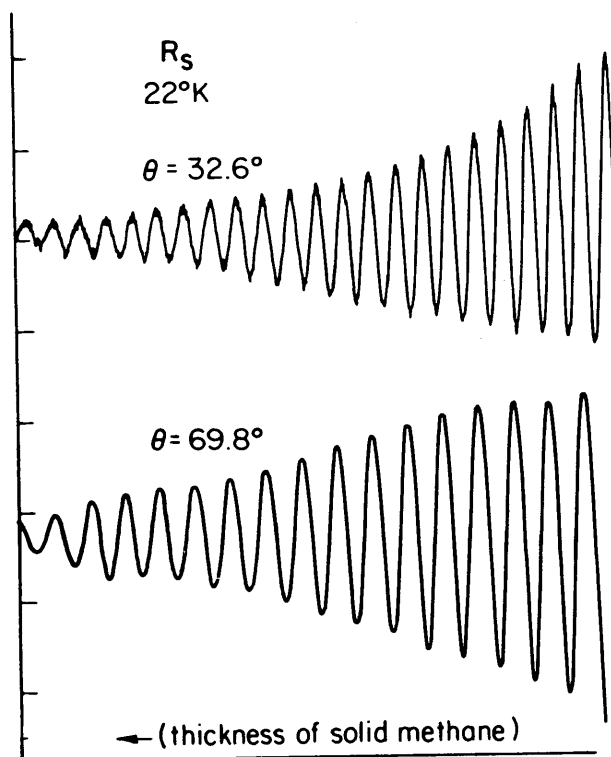


Fig. 6

beams is termed β , then

$$n = \frac{(\sin^2\theta_b - \beta^2\sin^2\theta_a)^{1/2}}{(1-\beta^2)^{1/2}} \quad (4)$$

where θ_a and θ_b are 32.6° and 69.8° , the two laser beam incidence angles. The index of refraction from the data in Fig. 6 gave $n = 1.302 \pm 0.002$ at $\lambda = 0.6328 \mu\text{m}$, confirming again that the value obtained by Lorentz-Lorenz relationship [Eq. (3)] is valid for CH_4 .

DISCUSSION AND CONCLUSIONS

Buie et al.¹⁷ have obtained photometric data of Pluto-Charon mutual events at wavelengths 1.53, 1.75, 2.00 and 2.35 μm while Sawyer³¹ has obtained data at wave-

lengths from 0.5 to 1.0 μm . This data allows the extraction of spectra of Pluto alone. Our optical constants from 1.1 to 2.63 μm (Table I and Fig. 3) and future determinations down to 0.4 μm are specifically useful in scattering models for Pluto, which are needed to determine how much CH_4 absorption arises from the surface and how much from the atmosphere.^{17,18,31} In a similar way, they can be used to model the texture and coverage of CH_4 on Triton.³²

Fink and Sill³³ have studied the reflection spectra of CH_4 frost at 60°K at a resolution of 11 cm^{-1} from 1.12 μm to 3.85 μm . They also determined transmission spectra through a film 7.1 μm thick, in the mid-IR from 2.63 μm to 20 μm , at 57°K and 72°K. Optical constants of CH_4 for this longer wavelength range could be estimated from that work, but are not computed explicitly here. Our k values are currently determined near band maxima for the near-IR 1.1 μm to 2.6 μm region. Attempts to measure k for CH_4 at shorter wavelengths (0.4-1.1 μm) by direct transmission are difficult due to scattering from surface imperfections. These surface scattering losses dominate the true extinction losses. To overcome this problem, we are investigating the possibility of using a double beam configuration, with a short pathlength through solid CH_4 in the reference beam and a long pathlength through solid CH_4 in the sample beam. This should largely cancel the scattering from the surface and thus allow the extraction of true transmission information.

Since the optical constants of CH_4 have application in a variety of planetary and cometary surface and atmospheric environments, we intend to measure optical constants for a wide variety of temperatures. Some work with C_2H_6 and C_2H_2 has been done, and studies of changes in the optical properties of CH_4 and other hydrocarbon ices after ultraviolet and charged particle irradiation are also planned.

ACKNOWLEDGEMENTS

This research is supported by NASA grants NGR 33-010-220, NGR 33-010-082, and NAGW 637, and by the Office of Health and Environmental Research, U.S. Dept. of Energy under Contract DE-AC05-84OR 21400 with Martin Marietta Energy Systems, Inc., ORNL.

References

1. B.N. Khare, C. Sagan, E.T. Arakawa, F. Suits, T. Callcott, and M. Williams, *Icarus* **60**, 127 (1984).
2. C. Sagan, W.R. Thompson, and B.N. Khare, *Proc. IAU Symp. 112*, edited by M.D. Papagiannis, p. 107, D. Reidel, Hingham, Mass. (1985).
3. C. Sagan, W.R. Thompson, S.W. Squyres, and B.N. Khare, *Bull. Amer. Astron. Soc.* **17**, 700 (1985).
4. C.P. McKay, J.B. Pollack, and R. Courtin, *Icarus* **80**, 23 (1989).
5. B.N. Khare, C. Sagan, W.R. Thompson, E.T. Arakawa, F. Suits, T.A. Callcott, M. W. Williams, S. Shrader, H. Ogino, T.O. Willingham, and B. Nagy, *Adv. Space Res.* **4**, 59 (1984).
6. K. Rages and J.B. Pollack, *Icarus* **41**, 119 (1980).
7. M.G. Tomasko and P.H. Smith, *Icarus* **51**, 65 (1982).
8. K. Rages and J.B. Pollack, *Bull. Amer. Astron. Soc.* **13**, 703 (1981).
9. K. Rages and J.B. Pollack, *Icarus* **55**, 50 (1983).
10. B.N. Khare, C. Sagan, W.R. Thompson, E.T. Arakawa, and P. Votaw, *J. Geophys. Res.* **92**, 15067 (1987).
11. C. Sagan and S.F. Dermott, *Nature* **300**, 731 (1982).
12. J.I. Lunine and D.J. Stevenson, in *Ice in the Solar System*, eds. J. Klinger, D. Benest, A. Dollfus, and R. Smoluchowski (Dordrecht: D. Reidel), pp. 741-757 (1985).
13. J.I. Lunine, D.J. Stevenson, and Y.L. Yung, *Science* **222**, 1229 (1983).
14. S.K. Atreya, *NASA Conference Publication 2330*, p. 55 (1984).
15. G.F. Lindel, J.R. Lyons, D.N. Sweetnam, V.R. Eshleman, D.P. Hinson, and G.L. Tyler, *J. Geophys. Res.* **92**, 14987 (1987).
16. D.P. Cruikshank and J. Apt, *Icarus* **58**, 306 (1984).
17. M.W. Buie, L.A. Lebofsky, E.F. Tedesco, and D.P. Cruikshank, *Bull. Am. Astron. Soc.* **21**, 985 (1989).
18. M.W. Buie and U. Fink, *Icarus* **70**, 483 (1987).
19. H.P. Larson, H.A. Weaver, M.J. Mumma, and S. Drapatz, *Astrophys. J.* **338**, 1106 (1989).
20. Cryocooler was Model LTS-22-Matrix-0.1 Closed Cycle Refrigerator System with Model CSD-3600 Si Diode Temperature Sensor obtained from Cryosystems, Inc., Tucson, AZ.
21. G.W.C. Kaye and T.H. Laby, *Tables of Physical and Chemical Constants*, pp. 83-86, Wiley, New York (1966).

22. N.J. Harrick, *Applied Optics* **10**, 2344 (1971).
23. K.R. Ramaprasad, J. Caldwell, and D.S. McClure, *Icarus* **35**, 400 (1978).
24. C.K.N. Patel, E.T. Nelson, and R.J. Kerl, *Nature* **286**, 368 (1980).
25. W.R. Thompson, *CRSR Report 918*, June 1989, Cornell University, Ithaca, NY.
26. L.P. Giver, *J. Quant. Spectrosc. Radiat. Transfer* **19**, 311 (1978).
27. E.T. Arakawa, P.D. Clapp, T.A. Calcott, B.N. Khare, and C. Sagan, *Bull. Am. Phys. Soc.* **31**, 700 (1986).
28. V.V. Sychev, A.A. Vasserman, V.A. Zagoruchenko, G.A. Spiridonov, and V.A. Tsymarny, *Thermodynamic Properties of Methane*, Hemisphere Publishing Corp., p. 175 (1987).
29. M.S. Constantino and W.B. Daniels, *J. Chem. Phys.* **62**, 3 (1975).
30. K.E. Tempelmeyer and D.W. Mills, *J. App. Phys.* **39**, 2968 (1968).
31. S.R. Sawyer, *Bull. Am. Astron. Soc.* **21**, 986 (1989).
32. W.R. Thompson, *Geophys. Res. Let.* **16**, 969 (1989).
33. U. Fink and G.T. Sill, *Comets*, ed. L.L. Wilkening, The University of Arizona Press, Tucson, Arizona, p. 164 (1982).